Chlorofluoroamines: Ab Initio and DFT Studies on Their Structure, Enthalpies of Formation, and Unimolecular Reaction Pathways

K. R. Shamasundar[†] and E. Arunan*

Department of Inorganic and Physical Chemistry, Indian Institute of Science, Bangalore 560 012, India

Received: April 10, 2001; In Final Form: July 10, 2001

Ab initio and density functional theory calculations are reported for the chlorofluoroamines HNXY (X/Y = F/Cl) and all possible unimolecular reaction products from their ground state. Reliable enthalpies of formation for these molecules and reaction products have been calculated using the G2 model. The large discrepancy between theory and experiment over the ΔH°_f(NCl) has been resolved by reevaluating the old experimental data. Optimized structures of all the species have been obtained at various levels up to MP2/6-311++G** and B3LYP/6-311++G**. The triplet−singlet energy gaps have been estimated for NH, NF and NCl at various levels. Enthalpies of various reactions have been calculated at advanced levels including PMP4, CBS-Q, G1, G2, and G2-MP2. Transition states (TS) for the three-centered HX elimination reactions have been characterized. Vibrational frequencies for all the reactants, products, and transition states have been calculated using HF, MP2 and DFT methods with 6-311++G** basis set. Threshold energies for the bond dissociation reactions and the HX (X = F/Cl) elimination reactions have been calculated. RRKM calculations have been carried out with these results to determine the branching ratio for the various possible reactions. The barrier for HCl elimination from HNFCl is 18 kcal mol^{-1} higher than that of HF elimination. Still, according to DFT results, it is found that the HCl elimination is an important channel because of entropy factors, possibly explaining the experimental observations. However, the MP2 and G2 results predict the HF elimination to be more important for HNFCl. Moreover, the N−Cl bond energies in HNFCl and $HNCl_2$ are less than the HCl elimination barriers. Hence, the as yet unsuspected N−Cl bond dissociation may be a dominant decomposition pathway for HNFCl and $HNCl_2$.

I. Introduction

Halogen amines are an interesting class of compounds whose chemical,[1−5] thermolytic,[6] and photolytic[7,8] reactions have been extensively studied. These compounds are, in general, very reactive and produce electronically excited species via both chemical and photolytic processes.[1] These excited species, particularly the excited state singlet nitrenes, can be successfully employed as a lasing medium.[9] These are among the few reactions in which dynamical constraints, such as conservation of spin angular momentum, dictate the formation of electronically excited species.

Reaction of hydrogen atom with halogen aminyl radicals[5,9−12] and quenching of NH(a) by halogens and interhalogens[13,14] are all believed to go through chemically activated halogen amines, HNXY (X/Y = F/Cl), in their singlet ground state.

$$H + NX_2\ (OR)\ NH(a) + X_2 \rightarrow HNX_2^* \rightarrow HX + NX(a\ ^1\Delta) \quad (1a)$$

$$\rightarrow HX + NX(X\ ^3\Sigma^-) \quad (1b)$$

$$\rightarrow HX + NX(b\ ^1\Sigma^+) \quad (1c)$$

For example, H + NF_2 reaction has a branching ratio of 0.91 for NF(a $^1\Delta$) channel[5,10] and the H + NCl_2 reaction gives NCl(a)/NCl(b) ratio of about 1000[1]. Both these experimental results could be qualitatively understood by assuming that HNX_2 is formed in the singlet state by addition followed by three-center elimination of HX to give NX(a $^1\Delta$). The NX(X $^3\Sigma^-$) ground state is spin forbidden, and the NX(b $^1\Sigma^+$) state is less favored due to higher energy. For these reactions the exit channel thermochemistry is reasonably established. However, the energetics of reagents and transition states are largely unknown. Because of the difficulty in preparation and their unstable nature, experimental data are hard to obtain. A comprehensive theoretical study on the unimolecular reactions of these haloamines has not been attempted, to the best of our knowledge. Except for a recent report on the HF elimination from HNF_2,[15] we are not aware of any theoretical work on the HX elimination from haloamines. Milburn et al. have reported theoretical enthalpies of formation for chloroamines (NH_mCl_n).[16] Mack et al. have reported ab initio studies on the structural aspects of fluoroamines (NH_mF_n).[17] On the other hand, studies on the analogous halomethanes are aplenty. Mulholland and Richards have reported a comprehensive semiempirical and ab initio study on HF elimination from various fluoromethanes.[18] Oref and Rabinovitch have reported model calculations on the decomposition of chlorofluoromethanes.[19] Several reports on the thermochemistry and bond energies of halomethanes have appeared over the years.[20−24]

The case of the chlorofluoroamine (HNFCl) is more interesting. The H + NFCl experimental results[2,4] could not be explained on the basis of an addition−elimination mechanism. The following reactions were considered (estimated enthalpy of reactions given in parentheses):[4]

* Author for communications. Email: arunan@ipc.iisc.ernet.in.
† Present address: National Chemical Laboratory, Pune, India 411008.

10.1021/jp011331g CCC: $20.00
Published on Web 08/25/2001

$$H + NFCl \rightarrow HNFCl^* \rightarrow NCl(a) + HF\ (-43) \quad (2a)$$

$$\rightarrow NF(a) + HCl\ (-14) \quad (2b)$$

If HNFCl intermediate is formed, the NCl(a) + HF channel should be the dominant one assuming that the HF/HCl elimination barriers follow the same order as the enthalpies of reactions and the preexponential factors are comparable. There are no experimental or theoretical estimates on these barriers or the nature of the transition states yet to verify these assumptions. However, the NF(a) + HCl channel was reported to be favored by factors of 3^4 and 10^1 compared to the NCl(a) + HF channel. It was speculated that the direct Cl abstraction may take place in the singlet surface.[4] However, the NH(a) + ClF reaction was also reported[14] to favor the NF(a) + HCl channel by a factor of 18 compared to the NCl(a) + HF channel. This reaction was thought to proceed by insertion as well and so the dominance of HCl elimination required a different explanation. In the case of analogous CF_2HCl (and other chlorofluoromethanes),[25] the HCl elimination is, in fact, favored by the thermochemistry unlike for HNFCl.

In this work, a systematic theoretical study of HX (X = F/Cl) elimination from HNF_2, HNFCl, and $HNCl_2$ has been carried out. Calculations have been carried out on all reactants, products (HNX, NXY, NX, and HX) and transition states for HX elimination. Enthalpies of formation for all the reactants, intermediates, products, and transition states have been calculated at the G2 level. All the bond energies have been computed for these haloamines in order to ascertain the importance of various unimolecular reactions. RRKM calculations have been carried out to determine the rates for the various channels. Comparison with the halomethanes brings out some important differences in bond energies and activation barriers for HX elimination between the haloamines and halomethanes. Throughout the paper, HF is used to denote both hydrogen fluoride and Hartree−Fock calculations. However, what is meant should be obvious from the context.

II. Computational Details

All Calculations have been performed with the GAUSSIAN-94 program suite.[26] Geometry optimizations have been carried out with the standard 6-31G** and 6-311++G** basis sets internally available in the program suite. Equilibrium and transition state geometries were fully optimized at the Hartee−Fock, second-order Møller−Plesset perturbation theory (UHF and UMP2, restricted for closed shell and unrestricted for open shell) with all the electrons correlated, and density functional theory using B3LYP correlation functional. All the transition states have been characterized with frequency analysis. Single-point calculations at fourth order Møller−Plesset perturbation theory (UMP4) with frozen core and density functional theory (DFT) with a large basis set, (6-311++G(2df,p)), were performed using geometries optimized at the UMP2/6-311++G-(d,p) and B3LYP/6-311++G(d,p) levels, respectively. Spin projection has been applied to annihilate the highest spin contaminant of the unrestricted wave function for the radicals. High accuracy methods such as CBS-Q and methods based on Gaussian-2 have been applied to reactants and products to get reliable information about the energetics of these systems. For the transition states, G1, G2, and G2(MP2) energies were calculated following Pople and co-workers' methodology.[27] Structural optimization was carried out at MP2(Full)/6-31G* level and the zero-point energies were calculated using vibrational frequencies determined by scaling HF/6-31G* results.

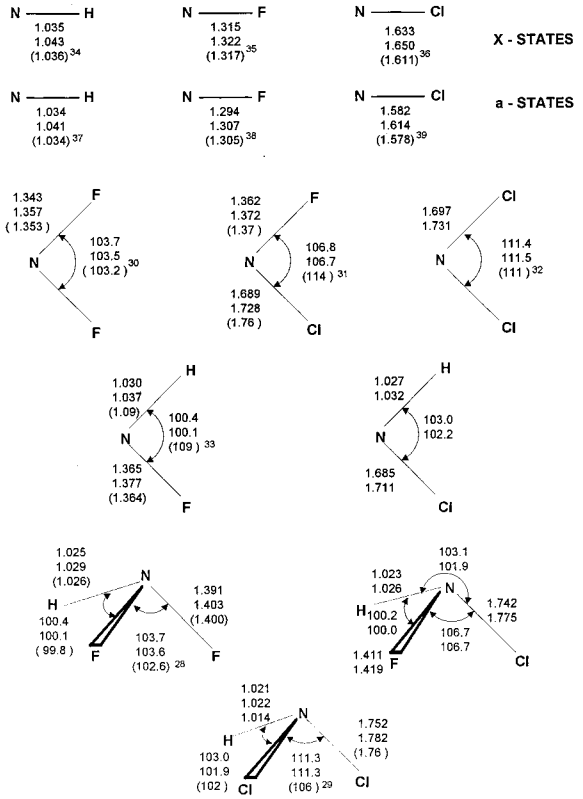

Figure 1. Structures of HNXY, HNX, NXY, NX and HY (X,Y = F,Cl) calculated at the MP2/6-311++G** (top) and B3LYP/6-311++G** (bottom) levels of theory. Experimental values, where available are given in parentheses with the references.

Zero-point energies have not been scaled except for high accuracy methods. All density functional theory calculations have been performed with B3LYP exchange−correlation functional.

III. Results and Discussion

III.1. Structure of Reactants and Products. The optimized structures for all reaction species at HF/6-31G**, HF/6-311++G**, MP2/6-31G**, MP2/6-311++G**, and B3LYP/6-311++G** levels of theory are given in Table 1S (Table numbers *X*S are to be found in the Supporting Information). Harmonic vibrational frequencies for all the species were calculated with HF, MP2, and DFT methods using 6/311++G** basis, and they are given in Table 2S. The structures are reproduced in Figure 1 where the MP2/6-311++G** and B3LYP/6-311++G** values are given along with the experimental results where available. For most of the species with experimentally determined structures, the HF level calculations led to deviations in the second decimal for distances in angstroms compared to deviations in the third decimals for MP2 and DFT level calculations. Moreover, the HF energies differed from experimental values by 20−50 kcal mol^{-1} (See section III.2), often leading to chemically unreasonable values such as an N−F bond energy of <10 kcal mol^{-1}. Hence, the HF results will not be included in the ensuing Discussion. For HNF_2 and $HNCl_2$, our results exactly agree with the ab initio results previously reported at the same levels.[16,17]

For HNF_2, the N−H distances calculated by MP2 and DFT methods are within 0.003 Å from the experimental value,[28] accurately determined from its rotational spectrum(1.026 Å). The same is true for the N−F distance calculated by DFT method but the deviation is 0.009 Å for the MP2/6-311++G**

level calculation. The deviation from the experiment is <1° for both ∠FNH and ∠FNF angles. For $HNCl_2$, experimental structure has been estimated using infrared spectra with several assumptions.[29] The N−H distance (in angstroms) was assumed to be the same as estimated for NH_2Cl (1.014) and our results (1.021) together with Milburn et al.'s[16] results on NH_2Cl (1.017) support this assumption. The N−Cl distance deduced from the infrared spectra is in very good agreement with the MP2 results but the DFT result for N−Cl distance is off by 0.02 Å. The ∠HNCl angle is predicted to within 1° by both methods but the ∠ClNCl angle differs from the experimental value by 5°. Interestingly, this angle is the same as that found in NCl_2 (111°) for which both experiment[32] and theory are in good agreement. In fact, for both F and Cl, the ∠HNX angle remains unchanged between HNX and HNXY at the same level of theory and the same is true for ∠XNY angle which remains unchanged for XNY and HNXY. It is likely that the experimental ∠ClNCl angle in $HNCl_2$ is an overestimate. For HNFCl, the experimental values are not available and from the above discussion, it can be concluded that the theoretical (MP2) bond angles are within 1° and the bond distances are within 0.01 Å from the actual values.

For aminyl radicals, unlike the bond angles that are nearly identical to the values found in the parent amine, the bond distances show large variations. For example, the N−F bond distance calculated at MP2/6-311++G** (experimental value in parentheses, references given in Figure 1) is 1.391(1.400), 1.411(−), 1.343(1.353), 1.362 (1.37), and 1.365(1.364) Å for HNF_2, HNFCl, NF_2, NFCl, and HNF, respectively. The downward trend from the amines to the aminyl radicals continues to the nitrenes and for NF, the distance at the same level is 1.315 (1.317) Å. The largest deviation is for NF_2 where the experimental N−F distance, precisely determined from its rotational spectrum,[30] is 0.01 Å longer than theoretical prediction. The DFT distances are uniformally larger by ≈0.01 Å than the MP2 ones, often blanketing the experimental results. The N−Cl distances show a similar trend. The N−H distances in all these species (HNXY, HNX, and NH) vary between 1.021 and 1.035 Å at MP2/6-311++G** level, but it increases from HNXY to HNX to NH, unlike the decrease observed in NF/NCl distances. The recent experimental N−H distance (1.09 ± 0.01 Å) in HNF has been estimated from the rotationally resolved fluorescence,[33] and it is 0.06 Å larger than the MP2/6-311++G** value. The experimental ∠HNF angle is much larger as well at 109° compared to the theoretical estimate of 100°. An earlier determination of the HNF structure, again from rotationally resolved electronic spectrum,[40] led to shorter NH distance (1.06 Å) and HNF angle (105°). Our results on NF_2 and HNF_2 are in closer agreement with the precisely determined experimental values. Hence, it appears that the experimental structure given for HNF[33] has larger uncertainty than what is reported. The ∠XNY bond angles for NF_2 and NCl_2 agree well with experimental values. For NFCl, the bond angle of 111° reported by Zarubaiko and Gilbert[31] appears to be too high. This structure was determined by doing normal coordinate analysis to fit the vibrational frequencies. As the authors point out, the bond angles in NXY are expected to follow the trend NF_2 < NFCl < NCl_2. Our theoretical results support this expectation. Accurate data on NFCl and NCl_2, based on microwave studies, are highly desirable but not available.

Nitrenes have received enormous attention over the years. Accurate experimental[34−39] and theoretical[41−44] results are available which are useful for comparison and validation. It is noted that the DFT distances are 0.01 Å or more larger than the MP2 distances for all nitrenes. Except for NF(a), MP2 results are closer to the experimental value than the DFT values. For NF(X) and NH(X and a), results at MP2/6-311++G** are within 0.002 Å from the experimental value but for NCl(X) the difference is 1 order of magnitude larger at 0.02 Å. Also, for NF(X) these results are in close agreement with the extensive CCSD(T) calculations using ccpVxZ (x = D,T,Q,5,6) basis sets.[41] However, for NCl(X), the latter results[41] show a significant improvement highlighting the need for including extensive correlation.

TABLE 1: Energetics of Various Unimolecular Reactions Channels for HNXY ($\Delta H°$ (0 K) in kcal mol^{-1}) Computed Using PMP4, B3LYP, CBS-Q, G1, G2-MP2, and G2 Methods

reaction system	PMP4[a]	B3LYP[b]	CBS-Q	G1	G2-MP2	G2	exptl[c]
HNF_2							
H + NF_2	00.0	00.0	00.0	00.0	00.0	00.0	00.0
HNF_2	−68.8	−69.4	−71.1	−72.4	−73.6	−73.5	−73.9
F + HNF	−04.7	−07.5	−06.7	−06.7	−06.8	−07.3	-
HF + NF(X)	−66.7	−66.4	−69.4	−68.0	−69.5	−69.5	−69.4
HF + NF(a)	−22.4	−20.9	−29.5	−30.0	−31.0	−31.0	−36.7
F_2 + NH(X)	+28.6	+30.1	+28.0	+27.6	+28.6	+28.4	25.3
F_2 + NH(a)	+79.8	+80.4	+68.8	+67.6	+69.1	+68.8	61.6
HNFCl							
H + NFCl	00.0	00.0	00.0	00.0	00.0	00.0	00.0
HNFCl	−73.0	−72.6	−75.4	−76.5	−77.5	−77.3	-
F + HNCl	−14.4	−16.1	−15.9	−15.1	−15.7	−16.1	-
Cl + HNF	−25.4	−27.9	−25.5	−25.6	−26.4	−27.2	-
HF + NCl(X)	−71.7	−72.3	−75.7	−73.0	−75.1	−75.1	−69.0
HCl + NF(X)	−54.0	−54.6	−55.1	−53.6	−55.8	−55.7	−46.0
HF + NCl(a)	−35.3	−34.6	−43.6	−42.7	−44.9	−44.7	−42.0
HCl + NF(a)	−09.7	−09.1	−15.2	−15.6	−17.3	−17.2	−13.0
ClF + NH(X)	−14.7	−13.2	−14.1	−14.8	−15.2	−15.9	−6.6
ClF + NH(a)	+36.5	+37.1	+26.7	+25.1	+25.3	+24.5	29.7
$HNCl_2$							
H + NCl_2	00.0	00.0	00.0	00.0	00.0	00.0	00.0
$HNCl_2$	−75.8	−74.5	−78.6	−78.9	−79.9	−79.7	−72
Cl + HNCl	−30.3	−32.7	−29.5	−29.8	−30.1	−31.2	-
HCl + NCl(X)	−54.2	−56.8	−56.1	−54.4	−56.1	−56.6	−56
HCl + NCl(a)	−17.8	−19.1	−24.0	−24.1	−25.9	−26.2	−29.5
Cl_2 + NH(X)	−26.4	−25.7	−25.7	−26.6	−25.8	−25.8	−24.8
Cl_2 + NH(a)	+24.8	+24.6	+15.1	+13.4	+14.7	+14.6	11.5

[a] Single-point energy at PMP4/6-311++(2df,p) with optimized geometry at MP2/6-311++G**. [b] Single-point energy at B3LYP/6-311++(2df,p) with optimized geometry at B3LYP/6-311++G**. [c] Experimental values are computed from data given in Table 2 along with references.

III.2. Thermochemistry of Reactants and Products. As has already been pointed out, the thermochemistry for H + NXY systems is largely unknown because of relative instability of these species at room temperature. Moreover, the available estimates have large and often uncertain error limits. Here, we report ab initio and DFT results for HNXY and all the possible products at various levels in a consistent manner.

To begin with, the thermochemistry of different channels for H + NXY reaction systems was calculated at HF and MP2 levels with 6-31G** and 6-311++G** basis sets and B3LYP/6-311++G** level. The H + NXY has been taken as the zero for energy to simplify the comparison with experiments. These results are presented in Table 3S. To improve the accuracy, single-point MP4/6-311++G(2df,p) and B3LYP/6-311++G-(2df,p) calculations were carried out with MP2/6-311++G** and B3LYP/6-311++G** optimized geometries, respectively. Moreover, calculations with CBS-Q, G1, G2-MP2 and G2 methods were carried out. The results of these calculations are shown in Table 1 along with experimental results where available. The enthalpies of formation ($\Delta H°_f$ at 0 K in kcal mol^{-1}) for all the species were calculated at G2 level, and these are given in Table 2.

TABLE 2: Enthalpies of Formation (in kcal mol^{-1}) Calculated with G2 Method and Experiment

molecule	G2, 0 K	expt	G2, 298.15 K	expt
HNF_2	−15.3	−14.0 ± 1.5	−16.9	−15.6 ± 1.5[a]
HNFCl	10.9		9.4	
$HNCl_2$	33.7		32.2	38 est[b]
NF_2	6.6	8.3 ± 0.5	6.0	7.9 ± 0.5[c]
NFCl	36.6	27 ± 6 est[m]	36.0	
NCl_2	61.8		61.4	58.4 est.[d]
HNF	32.4		31.7	25 ± 4 est[e]
HNCl	53.6		52.8	53.4 (theory)[b]
NH(X)	86.3	85.2 ± 0.4	86.3	85.2 ± 0.4[f]
NF(X)	54.9	55.6 ± 0.5	54.9	55.6 ± 0.5[c]
NCl(X)	79.3	62 ± 2, 75 ± 5	79.3	62 ± 2[g], 75 ± 5[h]
NH(a)	126.7	121.5 ± 0.4	126.7	121.5 ± 0.4[i]
NF(a)	93.4	88.3 ± 0.5	93.4	88.3 ± 0.5[i]
NCl(a)	109.6	101.5 ± 5	109.6	101.5 ± 5[i]
HF	−66.2	−65.1 ± 0.2	−66.2	−65.1 ± 0.2[j]
HCl	−22.4	−22.02 ± 0.05	−22.4	−22.06 ± 0.05[j]
F_2	0.3	0.0	0.3	0.0[k]
ClF	−13.9	−13.2 ± 0.2	−14.0	−13.2 ± 0.2[l]
Cl_2	1.4	0.0	1.4	0.0[k]

[a] Reference 46. [b] Reference 16. [c] Reference 48. [d] Reference 49. [e] Reference 50. [f] Reference 51. [g] Reference 52. [h] Experimental value from ref 52 is revised on the bases of newer enthalpy data available for N_3, refs 53 and 54; see text. [i] S−T gap from Table 2 is added to the triplet state enthalpy of formation. [j] Reference 47. [k] Standard state. [l] Reference 27. [m] Reference 4.

TABLE 3: Triplet−Singlet Energy Spacing (in kcal mol^{-1}) for NX (X = F, Cl) Calculated at Different Levels of Theory[a]

method	NH	NF	NCl
MP2/6-31G**	58.2	49.7	43.5
MP2/6-311++G**	55.7	49.2	41.6
B3LYP/6-311++G**	50.5	45.8	39.6
PMP4[b]	51.2	44.3	36.4
B3LYP[c]	50.3	45.5	37.7
CBS-Q	40.8	39.9	32.1
G1	40.0	38.0	30.3
G2-MP2	40.5	38.5	30.2
G2	40.4	38.5	30.4
MRD-CI	37.3[d]	31.6[e]	30.4[f]
exptl	36.2[g]	32.7[h]	26.5[i]

[a] Experimental values are also indicated. There is no uncertainty within the quoted decimals for the experimental values. [b] Single-point energy at PMP4/6-311++(2df,p) with optimized geometry at MP2/6-311++G**. [c] Single-point energy at B3LYP/6-311++(2df,p) with optimized geometry at B3LYP/6-311++G**. [d] Reference 44. [e] Reference 42. [f] Reference 43. [g] Reference 37. [h] Reference 60. [i] Reference 45.

The HNXY molecules have singlet ground state and the HX elimination channels correlate to NY(a) singlet state. Hence, it was necessary to determine the energies of both the NY(X) triplet ground and the NY(a) singlet excited states. The singlet−triplet (S−T) energy gaps predicted with all these methods are given in Table 3, along with results from very advanced level (MRCI) calculations available in the literature. The data given in Tables 2 and 3 clearly identify one problem with different levels of theory. The S−T gap predicted is higher than the experimental value (in kcal mol^{-1}) by 25−35 at HF level (not shown in Table), 10−15 at MP2 and DFT levels, and 4−6 at the more advanced levels. The $\Delta H°_f$ calculated for the ground-state triplet nitrenes at G2 level are in very good agreement with experiment and higher level calculations for NF[43] and NH[44] but differs from the experimental NCl value by 17 kcal mol^{-1}. The only experimental estimate on $\Delta H°_f$ reported for NCl is 62 ± 2 kcal mol^{-1} by Clark and Clyne.[52] This estimate was based on observing the NCl(b → X) chemiluminescence from the following reaction:

$$Cl + N_3 \rightarrow NCl(b) + N_2 \quad (3)$$

The maximum vibronic energy observed in the product NCl sets an upper limit to the exothermicity of the reaction. The $\Delta H°_f$ for N_3 was estimated similarly by the NO/N_2 emission from

$$O/N + N_3 \rightarrow NO/N_2 + N_2 \quad (4)$$

reactions with known values of $\Delta H°_f$ for O, N and NO. This method can give only a lower limit for the $\Delta H°_f$ of N_3 and it was assigned as 99 kcal mol^{-1}. The $\Delta H°_f$ (N_3) has been revised upward by two groups later. By observing the HF(v,J) infrared chemiluminescence (IRCL) from F + HN_3, Setser and co-workers[53] estimated a value of ≤113.6 kcal mol^{-1}. Using ion cyclotran resonance technique, Brauman and co-workers[54] determined $\Delta H°_f$ of N_3 to be 112 ± 5 kcal mol^{-1}, in close agreement with IRCL estimate. Using this revised estimate for $\Delta H°_f(N_3)$, the $\Delta H°_f$ (NCl) is reevaluated to be 75 ± 5 kcal mol^{-1}, in reasonable agreement with the G2 value of 79.3. The more accurate theoretical estimate of Xantheas et al.[41] based on CCSD(T) and MRCI calculations predict $\Delta H°_f$ for NCl to be 76.5 kcal mol^{-1}, in better agreement with the experiment. Here, it should be pointed out that Clyne's estimate for NCl is also a limit and not an absolute measurement. However, on the basis of the agreement between theory and experiments for many of the systems considered here, it is concluded that the experimental $\Delta H°_f$ for NCl is well established at 75 ± 5 kcal mol^{-1}.

In the following discussion about the G2 results, one should keep in mind that the NX singlet states are overestimated by up to 6 kcal mol^{-1}. This is important when analyzing the enthalpies and barriers for the HX elimination reactions on the singlet potential energy surface. The results for HNF_2, HNFCl, and $HNCl_2$ and their reaction products are discussed individually followed by a comparative summary below.

III.2.a. HNF_2. The experimental $\Delta H°_f$ for HNF_2 and most of its reaction products (NF_2, NH, NF, HF, F_2, H, and F) are well established except for HNF. These are included in Table 2. For HNF an estimate[50] of 25.5 ± 4 kcal mol^{-1} based on the then available N−F and N−H bond dissociation energies in the NF and NH diatomics coupled with CI calculations on HNF is available. For all these species except HNF the G2 values are within 1−2 kcal mol^{-1}, the largest deviation being 1.7 kcal mol^{-1} for NF_2 at 0 K. The G2 $\Delta H°_f$ reported here for HNF (32.4 at 0 K) should be accurate to 2 kcal mol^{-1} or better. The agreement in Table 2 suggests that the G2 thermochemistry given in Table 1 should be accurate to 1−2 kcal mol^{-1} for reactions producing all ground-state products but for the reactions leading to excited states the error can be ≥5 kcal mol^{-1}. From Table 1, it is clear that the G2 and G2-MP2 results differ by less than 1 kcal mol^{-1} for all reactions considered. The G1 and CBS-Q results are within 1−2 kcal mol^{-1} from the G2 estimates. For single-point MP4 and B3LYP calculations, the differences from G2 values are larger at 4−5 kcal mol^{-1}.

III.2.b. $HNCl_2$. For $HNCl_2$ and its chlorine containing products, accurate experimental $\Delta H°_f$ are not available. For $HNCl_2$ and NCl_2 some indirect estimates, with unknown error limits, are available and they differ from the G2 value by 6 and 3 kcal mol^{-1}, respectively. For HNCl, there is no experimental determination available. Milburn et al.[16] have reported single-point MP4 and QCISD(T) calculations with MP2 optimized geometry for all NH_mCl_n species with the same large basis set, 6-311++G**. Their results are in very good agreement with the G2 values reported here for $HNCl_2$, HNCl, NCl_2, NH, and

TABLE 4: Energy Barriers (in kcal mol^{-1}) for Various Reactions from HNXY

reaction system	MP2/6-31G**	MP2/6-311++G**	B3LYP/6-311++G**	PMP4[a]	B3LYP[b]	G1	G2	G2(MP2)
HNF_2								
$HNF_2 \rightarrow NF(a) + HF$	56.1	53.7	46.2	50.6	47.8	50.4	50.9	51.2
$HNF_2 \rightarrow F + HNF$	64.7	61.8	59.2	64.1	61.9	65.7	66.2	66.8
HNFCl								
$HNFCl \rightarrow NCl(a) + HF$	51.9	48.0	39.7	43.4	40.0	43.1	42.8	43.0
$HNFCl \rightarrow NF(a) + HCl$	68.0	66.4	58.2	63.3	60.1	60.9	60.9	60.8
$HNFCl \rightarrow F + HNCl$	60.9	59.4	55.1	58.6	56.5	61.4	61.2	61.8
$HNFCl \rightarrow Cl + HNF$	44.6	45.0	41.7	47.6	44.7	50.9	50.1	51.1
$HNCl_2$								
$HNCl_2 \rightarrow NCl(a) + HCl$	64.1	61.4	51.2	56.9	51.5	57.6	56.9	56.8
$HNCl_2 \rightarrow Cl + HNCl$	44.6	46.0	39.7	45.5	41.8	49.1	48.5	49.8

[a] Single-point energy at PMP4/6-311++(2df,p) with optimized geometry at MP2/6-311++G**. [b] Single-point energy at B3LYP/6-311++(2df,p) with optimized geometry at B3LYP/6-311++G**.

NCl. The accuracy of the other methods compared to G2 is similar to what is discussed above for HNF_2.

III.2.c. HNFCl. For HNFCl and its products the thermochemistry is virtually unknown. The experimental results given in Tables 1 and 2 are estimates from ref 4 and they differ from the G2 predictions by up to 9 kcal mol^{-1}. The ΔH^o_f for NFCl (Table 2, 27 kcal mol^{-1}) seems to be the major cause for this difference. This estimate was made by assigning the N−Cl bond energy in NFCl as 57 kcal mol^{-1} based on several assumptions about the N−Cl bond energies in NFCl, NCl_2, $NFCl_2$, and NCl_3. From the G2 ΔH^o_f listed in Table 4, the N−Cl bond energy in NFCl is calculated to be 47 kcal mol^{-1} only. The ΔH^o_f for HNFCl has not been reported earlier to the best of our knowledge and the value calculated at the G2 level is very close to the average of ΔH^o_f for HNF_2 and $HNCl_2$, which is reasonable.

III.2.d. General Observations. The N−H bond energy increases in the order HNF_2 < HNFCl < $HNCl_2$ at all levels of calculations. Substitution of Cl for F leads to an increase in N−H bond energy, and this is the opposite of what is observed in halomethanes.[55] At the G2 level the N−H bond energies are 73.5, 77.3, and 79.7 for the three haloamines compared to 106.4 kcal mol^{-1} for NH_3[27], a huge 30 kcal mol^{-1} reduction on halogen substitution. Baumgartel et al.[56] have noted such drastic reduction in N−H bond energies on going from NH_3 to NH_2F to NHF_2. Milburn et al.[16] have noted similar trends for NH_3, NH_2Cl, and $NHCl_2$. Halogen substitution does alter the C−H bond energies but F and Cl have opposite effect. Moreover, the effect is much smaller. The C−H bond energies in CH_4, CF_3H, and CCl_3H are 105, 107 and 96, respectively.[55] Almost all the chlorofluoromethanes have C−H bond energies[55] between 95 and 105 kcal mol^{-1}. Another interesting observation is that the bond energies increase in the order N−Cl < N−F < N−H in all three haloamines. At the G2 level, the N−F (N−Cl) bond in HNF_2 ($HNCl_2$) is weaker by 7(31) kcal mol^{-1} compared to the N−H bond. Again, it is different from the halomethanes for which one finds the bond energies to increase in the order C−Cl < C−H < C−F.[55]

III.3. Transition States for Unimolecular Elimination Reactions. Optimized transition state (TS) geometries at various levels of calculations are given in Table 4S. Frequency calculations were performed at HF, DFT, and MP2 levels with 6-311++G** basis set for the saddle points (TS), and they are given in Table 4. The HF frequencies have been included in this table, as the G2 method used the scaled HF frequencies in thermochemical calculations. The structures of the transition states are shown in Figure 2. Energy barriers at various levels of theory are listed in Table 5. The schematic energy level diagram for the H + NF_2/NFCl reaction is given in Figure 3.

All the transition states are geometrically closer to products than to reactants i.e., cases of late barrier. Significant changes are observed between HF, MP2, and B3LYP optimized TS geometries. Such a trend between HF and MP2 was observed in our earlier work on HCl elimination from CH_3COCl.[57] With MP2 and B3LYP methods, the TS move much closer toward products compared to the HF level. For example, at B3LYP/6-311++G** level, the HF (HCl) distance in HNFCl is 1.890 (2.225) Å compared to 1.187 (1.300) Å in the TS connecting to HF + NCl (HCl + NF). The HF (HCl) bond distance at this level is 0.922 (1.287) Å. The N−H bond is partially broken but the N−X bond is almost completely broken. This is very similar to the HX elimination TS found for halomethanes,[18,57,58] where the C−H bond is partially broken and the C−X bond is more fully broken. However, HX elimination transition states

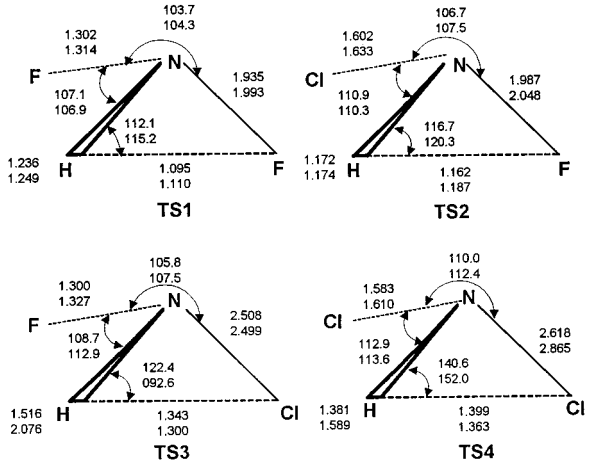

Figure 2. Structure of the transition states for HX elimination from HNXY calculated at the MP2/6-311++G** (top) and B3LYP/6-311++G** (bottom) levels of theory. TS1 and TS2 are for HF elimination from HNF_2 and HNFCl, respectively. TS3 and TS4 are for HCl elimination from HNFCl and $HNCl_2$, respectively.

TABLE 5: Frequencies of Optimized Transition State for Unimolecular HX (X = F, Cl) Elimination from HNXY

reaction[a]	HF/ 6-311++G**	MP2/ 6-311++G**	B3LYP/ 6-311++G**
$HNF_2 \rightarrow$	1911i, 324, 607	1426i, 292, 633	1094i, 259, 530
$NF^1(a) + HF^2$	1300, 1439, 2498	1167, 1241, 2086	1127, 1220, 1924
HNFCl →	1808i, 262, 527	1449i, 243, 623	1144i, 209, 511
NCl(a) + HF	879, 1279, 2553	909, 1206, 2103	832, 1197, 1964
HNFCl →	1581i, 216, 433	626i, 182, 317	311i, 106, 251
NF(a) + HCl	1166, 1261, 1749	764, 1178, 2105	283, 1096, 2781
$HNCl_2 \rightarrow$	1495i, 167, 329,	587i, 149, 578	172i, 104, 505
$NCl^1(a) + HCl^2$	866, 1119, 1660	915, 956, 1469	773, 868, 1838

[a] Superscript 2 is used on halogen atom being eliminated, in the case of ambiguity.

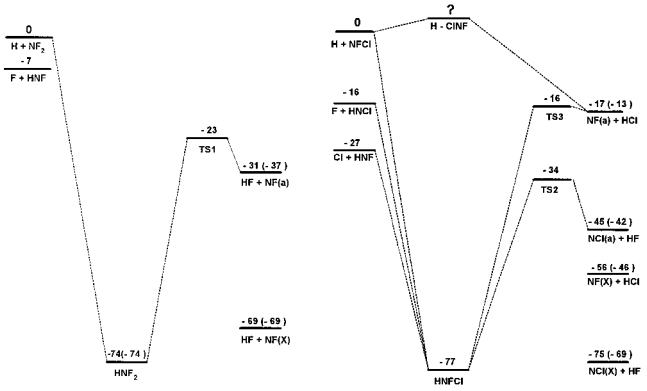

Figure 3. Schematic energy level diagram of the H + NF_2 and H + NFCl reactions. The values given are at G2 level. For other values see Tables 1 and 3S. Experimental values are given in parentheses where available. (See Table 2 for references).

with long C−X bond lead to significantly larger preexponential factors than what has been observed experimentally for haloalkanes.[58]

A dramatic change in N−H distance in the TS for HCl elimination from HNFCl is observed when going from HF (1.25 Å) to MP2 (1.51 Å) to DFT (2.08 Å) level calculation. For comparison, the N−H distances in the TS for HF elimination from HNF_2 and HNFCl change by ≤0.1 Å between different levels. Among bond angles, major changes are observed in ∠XHN, which increases upon inclusion of correlation with MP2 and DFT methods. Within each level, the TS geometries and frequencies are somewhat insensitive to basis set. Another notable feature is that the X−H−N−Y dihedral angle is almost constant for all TS.

An analysis of the normal-mode frequencies of TS confirms that the transition state structure becomes much looser upon inclusion of correlation. The TS for HCl elimination is looser than HF elimination at all levels. The loosest TS are obtained with the DFT method. For all TS, the mode corresponding to the reaction coordinate is dominated by the NH stretch with minor contribution from the halogen atoms. The relative motion of the four atoms involved confirms the correctness of the TS for the given reaction. It can be inferred that elimination reactions proceed by complete breaking of the NX bond along with concomitant formation of the HX bond. In the process, the NH bond is significantly weakened. The final stage of elimination proceeds through complete breaking of the partially broken NH bond. The DFT results for HCl elimination from $HNCl_2$ is different from the others with significant and nearly equal amplitudes for H, N, and the Cl being eliminated. The imaginary frequency, which corresponds to the reaction coordinate, at the TS for HCl elimination from $HNCl_2$ changes from 1495 at HF level to 587 at MP2 and 172 cm^{-1} in DFT calculations. For HF elimination from HNF_2, the imaginary frequency changes less dramatically from 1911 at HF level to 1426 at MP2 and 1094 cm^{-1} in DFT calculations. The results for HF/HCl elimination from HNFCl resemble that of HNF_2/$HNCl_2$, respectively. The very low imaginary frequency for HCl elimination from DFT calculations predict that tunneling may not be significant. On the other hand, for HF elimination with higher imaginary frequency, tunneling could be important. There is no direct or indirect experimental data on the transition states such as thermal rate constants and preexponential factors for these systems. Hence, there appears to be no basis on which one could evaluate the different predictions from HF, MP2, and DFT calculations. (However, see next section on the branching ratio from RRKM calculations.)

The energy barriers for various elimination reactions presented in Table 4 reveal that the barrier energies are much less than the corresponding N−H bond energies. This suggests that the H + NXY → HX + NY(a) reactions can go through HNXY intermediate as assumed in all the experimental work so far. The G2 values for the barriers differ from the MP2 and B3LYP values by 3−6 kcal mol^{-1}. The PMP4 and B3LYP single-point calculations with the larger basis set reduces the difference from G2 value to 0−3 kcal mol^{-1}. The convergence of the barrier heights at these high level calculations suggest that the transition states have been well characterized.

It can be noticed that the barrier for HCl elimination is higher than that for HF elimination in haloamines. This is in sharp contrast to the halomethanes for which the HF elimination has a larger barrier than the HCl elimination.[25] It is mostly due to the stability of the fluorocarbenes most of which have negative $\Delta H°_f$ compared to that of NF. The HF elimination barrier decreases with the presence of more Cl atoms whereas the presence of more F atoms increases the barrier for HCl elimination.

III.4. RRKM Calculations on HX Elimination from HNXY. To determine the relative importance of the HF and HCl elimination channels, RRKM calculations were carried out, as described in ref 57. Calculations used structure, vibrational frequencies, and energetics determined at the G2, MP2, and DFT levels. For G2 level calculations Hartree−Fock frequencies and MP2 optimized structures were used. The unimolecular rate constants for HF and HCl elimination reactions were calculated at $\langle E \rangle$ corresponding to H + NFCl and NH(a) + FCl entrance channels. The results are given in Table 6. The HX elimination reactions from all three haloamines are predicted to occur in picosecond time scale at these energies.

The rate constants calculated at different levels follow the trend MP2 < G2 < DFT. The G2 values are larger than MP2 values mainly due to the energetics. However, the DFT rate constants are larger due to frequency factors, as expected from the nature (looseness) of the TS calculated at these levels. The DFT results for the H + NFCl and NH(a) + ClF reactions are intriguing. The barrier for HCl elimination is about 20 kcal mol^{-1} higher than that for the HF elimination. However, the TS for HCl is much looser than that for the HF elimination. The latter effect dominates the RRKM rate constants. At the MP2 level, the HF elimination rate is 10 times faster than the HCl elimination. But at the DFT level, both these reactions have comparable rates differing by a factor of 2 only. For the NH(a) + ClF insertion reaction, the HNFCl intermediate would have available energy about 110 kcal mol^{-1}. At these energies, the HCl elimination rate is 2.5 times faster than the HF elimination. Thus, the DFT results are in qualitative agreement with the experimental observations from both the H + NFCl[4] and NH(a) + ClF[14] reactions. However, as is evident from Figure 3, the N−X bond dissociation reactions need to be considered to assess the overall importance of these molecular elimination reactions and they are discussed next.

III.5. N−X Dissociation Reactions for HNXY. The N−F bond energy in HNF_2 is found to be 8−14 kcal mol^{-1} higher than the HF elimination barrier in MP2 and DFT level calculations (Table 5), the higher limit favored by the advanced calculations. Hence, for the H + NF_2 reaction, the HF elimination is expected to be the most important channel. For the NH(a) + F_2 reaction, with the available energy of about 150 kcal mol^{-1}, the F + HNF reaction will become important.

TABLE 6: RRKM Rate Constants for the Unimolecular HX Elimination from HNXY[a]

molecule	$\langle E\rangle$ (MP2) kcal mol^{-1}	k (MP2) s^{-1}	$\langle E\rangle$ (DFT) kcal mol^{-1}	k (DFT) s^{-1}	$\langle E\rangle$ G2 kcal mol^{-1}	k(G2) s^{-1}
HNF_2	70	1.01×10^{12}	70	5.69×10^{12}	74	4.15×10^{12}
HNFCl (HF)	75	1.75×10^{12}	73	5.63×10^{12}	78	7.09×10^{12}
	115	1.25×10^{13}	110	2.42×10^{13}	103	2.05×10^{13}
HNFCl (HCl)	75	1.13×10^{11}	73	2.57×10^{12}	78	7.41×10^{11}
	115	1.05×10^{13}	110	6.54×10^{13}	103	7.66×10^{12}
$HNCl_2$	80	7.31×10^{11}	76	3.96×10^{12}	80	4.00×10^{12}

[a] $\langle E\rangle = 75$ corresponds to available energy from H + NFCl and $\langle E\rangle = 115$ corresponds to NH(a) + ClF.

The bond dissociation reactions usually have larger preexponential factors,[57] and they become more important at higher energies.

The situation for HNFCl appears to be more complicated. As expected, the HF elimination has the lowest barrier. However, the N−Cl bond energy in HNFCl is very close to this barrier. At MP2 level, the N−Cl bond energy is in fact smaller than the barrier for HF elimination. Advanced level calculations reverse this trend, and at the G2 level the HF elimination barrier is 8 kcal mol^{-1} lower than the N−Cl bond energy. On the other hand, the barrier for HCl elimination from HNFCl is 10 kcal mol^{-1} above the N−Cl bond energy. This should suggest that the N−Cl dissociation will be competing with HF elimination and it will be more dominant than the HCl elimination from HNFCl. However, as already pointed out, the barrier for HCl elimination may be overestimated by 5−6 kcal mol^{-1}. In any case, it can be concluded that the N−Cl dissociation leading to HNF + Cl from HNFCl may be an important channel if not more important than HCl elimination. So far, there has been no experimental attempt to look for HNF from the H + NFCl or NH(a) + ClF reaction.

The case of $HNCl_2$ is similar to that of HNFCl as can be inferred from Table 4. Results of calculations at all the levels predict the N−Cl dissociation to be more important than HCl elimination. Here again, there has been no attempt to detect HNCl from either the H + NCl_2 or NH(a) + Cl_2 reaction. It is likely that both HCl elimination and N−Cl dissociation occur, but only the HCl elimination channel has been observed experimentally.

The H + NCl_2/NFCl reaction could go through direct Cl abstraction in the singlet or triplet channel. Guo and Deng[59] have considered the F abstraction from the triplet channel for H + NF_2. They find that the barrier for F abstraction in triplet channel is 20.6 kcal mol^{-1} at MP2/6-31G* level and hence rule out this possibility. Singlet channel abstraction has not been explored yet. In general, Cl abstraction reactions have lower barrier than the F abstraction reactions. Hence, Cl abstraction through the singlet and triplet potential surface for both H + NFCl and H + NCl_2 need to be explored and such studies are planned. Also, exit channel interactions in the N−Cl dissociation process could lead to the thermodynamically favored HCl channel through "secondary encounters" .

IV. Summary and Conclusions

The haloamines, HNXY, and their unimolecular reactions' products along with the transition states for HX elimination have been investigated by ab initio and DFT calculations. The important findings from this study are summarized below.

(1) The HF level calculations are very inadequate for haloamines. Inclusion of correlation at the MP2 or DFT level improves the results significantly.

(2) Enthalpies of formation for all the reactants and products have been reported at the G2 level. For the ground states the uncertainty is expected to be less than 3 kcal mol^{-1}. The experimental $\Delta H°_f$ (NCl(X)) is reevaluated to be 75 ± 5 kcal mol^{-1}, resolving the large discrepancy between the theory and experiment that existed in the literature. Structure and vibrational frequencies for all the reactants, products and TS have been reported at HF, MP2, and DFT levels.

(3) For the haloamines, the bond energies increase in the order N−Cl < N−F < N−H. Halogen substitution lowers the N−H bond energy drastically. Among the three haloamines studied, the N−H bond energy increases in the order HNF_2 < HNFCl < $HNCl_2$.

(4) The HX elimination from the haloamines proceeds through a loose, product like, TS resembling similar TS found for HX elimination from halomethanes. The barrier for HF elimination from haloamines reduces on Cl substitution whereas the HCl elimination barrier increases on F substitution. The barrier for HCl elimination is 18 kcal mol^{-1} larger than that of HF elimination for HNFCl. However, entropy factors seem to favor HCl elimination, especially at high energies.

(5) For HNFCl and $HNCl_2$, the calculated N−Cl bond energies are less than the barrier for HCl elimination, suggesting that N−Cl dissociation may be more important in these reactions.

Acknowledgment. We acknowledge fruitful discussions with Prof. S. Manogaran (IIT, Kanpur), Prof. J. Chandrasekhar, and Prof. K. L. Sebastian(IISc, Bangalore). This work started as an M.Sc. project of K.R.S. in IIT Kanpur when E.A. was working there. We thank Prof. D. W. Setser for critical comments on an earlier version of the manuscript and for referring us to the newer enthalpy data for N_3. We thank Mr. Dharmendar Ramdoss for help with Figures. We thank Supercomputer Education and Research Center of the IISc and the Computer Center in IIT, Kanpur for providing the necessary computational environment.

Supporting Information Available: Table 1S. Optimized ground-state geometries for HNXY and various reaction fragments calculated at HF/6-31G**, HF/6-311++G**, MP2/6-31G**, MP2/6−11++G**, and B3LYP/6-311++G** levels of theory with experimental values where available. Table 2S. List of vibrational frequencies (in cm^{-1}) for HNXY and various fragments calculated at HF, MP2 and DFT levels with 6-311++G** basis set. Table 3S. Enthalpies of various unimolecular reactions for HNXY ($\Delta H°$ (0 K) in kcal mol^{-1}) computed using HF, MP2, and DFT methods given in Table 1S. Table 4S. Optimized transition state geometries for unimolecular HX (X = F, Cl) elimination from HNXY at various levels of theory as given in Table 1S. This material is available free of charge via the Internet at http://pubs.acs.org.

References and Notes

(1) Exton, D. B.; Gilbert, J. V.; Coombe, R. D. *J. Phys. Chem.* **1991**, *95*, 2692.

(2) Exton, D. B.; Gilbert, J. V.; Coombe, R. D. *J. Phys. Chem.* **1991**, *95*, 7758.
(3) Exton, D. B.; Williams, S. A.; Gilbert, J. V. *J. Phys. Chem.* **1993**, *97*, 4326.
(4) Arunan, E.; Liu, C. P.; Setser, D. W.; Gilbert, J. V.; Coombe, R. D. *J. Phys. Chem.* **1994**, *98*, 494.
(5) Malins, R. J.; Setser, D. W. *J. Phys. Chem.* **1981**, *85*, 1342.
(6) Gershanovich, Y. I.; Gilbert, J. V. *J. Phys. Chem. A.* **1997**, *101*, 840.
(7) Gilbert, J. V.; Wu, X. L.; Stedman, D. H.; Coombe, R. D. *J. Phys. Chem.* **1987**, *91*, 4265.
(8) Conklin, R. A.; Gilbert, J. V. *J. Phys. Chem.* **1990**, *94*, 3027.
(9) Ray, A. J.; Coombe, R. D. *J. Phys. Chem.* **1995**, *99*, 7849.
(10) Heidner, R. F.; Helvajian, H.; Holloway, J. S.; Koffend, J. B. *J. Phys. Chem*. **1989**, *93*, 7818.
(11) Herbelin, J. M.; *Chem. Phys. Lett.* **1976**, *42*, 367.
(12) Herbelin, J. M.; Cohen, N. *Chem. Phys. Lett.* **1973**, *20*, 605.
(13) Singleton, S. M.; Coombe, R. D. *Chem. Phys. Lett*. **1993**, *215*, 237.
(14) Singleton, S. M.; Coombe, R. D. *J. Phys. Chem.* **1995**, *99*, 16296.
(15) Guo, J.-Z.; Deng, C.-H. *Gaodeng Xuexiao Huaxue Xuebao* (Chinese) **1996**, *17*, 1904.
(16) Milburn, R. K.; Rodriquez, C. F.; Hopkinson, A. C. *J. Phys. Chem. B.* **1997**, *101*, 1837.
(17) Mack, H.-G.; Christen, D.; Oberhammer, H. *J. Mol. Struct*. **1988**, *190*, 215.
(18) Mulholland, A. J.; Richards, W. G. *Int. J. Quantum. Chem.* **1994**, *51*, 161.
(19) Oref, I.; Rabinovitch, B. S. *J. Phys. Chem.* **1977**, *81*, 2587.
(20) Ignacio, E. W.; Schlegel, H. B. *J. Phys. Chem.* **1992**, *96*, 5830.
(21) Berry, R. J.; Burgess, D. R. F., Jr.; Nyden, M. R.; Zachariah, M. R.; Melius, C. F.; Schwartz, M. *J. Phys. Chem.* **1996**, *100*, 7405.
(22) McGiven, W. S.; Derecski-Kovacs, A.; North, S. W.; Fransisco, J. S. *J. Phys. Chem. A.* **2000**, *104*, 436.
(23) Haworth, N. L.; Smith, M. H.; Bacskay, G. B.; Mackie, J. C. *J. Phys. Chem. A.* **2000**, *104*, 7600.
(24) Rodriquez, C. F.; Bohme, D. K.; Hopkinson, A. C. *J. Phys. Chem.* **1996**, *100*, 2942.
(25) Arunan. E.; Rengarajan. R.; Setser. D. W. *Can. J. Chem.* **1994**, *72*, 568.
(26) Frisch, M. J.; Trucks, G. W.; Schlegel, H. B.; Gill, P. M. W.; Johnson, B. G.; Robb, M. A.; Cheeseman, J. R.; Keith, T.; Petersson, G. A.; Montgomery, J. A.; Raghavachari, K.; Al-Laham, M. A.; Zakrzewski, V. G.; Ortiz, J. V.; Foresman, J. B.; Cioslowski, J.; Stefanov, B. B.; Nanayakkara, A.; Challacombe, M.; Peng, C. Y.; Ayala, P. Y.; Chen, W.; Wong, M. W.; Andres, J. L.; Replogle, E. S.; Gomperts, R.; Martin, R. L.; Fox, D. J.; Binkley, J. S.; Defrees, D. J.; Baker, J.; Stewart, J. P.; Head-Gordon, M.; Gonzalez, C.; Pople, J. A. *Gaussian 94*, revision C.2; Gaussian, Inc.: Pittsburgh, PA, 1995.
(27) Curtiss, L. A.; Raghavachari, K.; Redfern, P. C.; Pople, J. A.; *J. Chem. Phys*. **1997**, *106*, 1063 and references therein.
(28) Lide, D. R. *J. Chem. Phys.* **1963** *38*, 456.
(29) Moore, G. F.; Badger, R. M. *J. Am. Chem. Soc.* **1952**, *74*, 6076.
(30) Brown. R. D.; Burden. F. R.; Godfrey. P. D.; Gillard. I. R. *J. Mol. Spectrosc*. **1974**, *52*, 301.
(31) Zarubaiko, A. M.; Gilbert. J. V. *J. Phys. Chem.* **1993**, *97*, 4331.
(32) Kohlmiller, C. K.; Andrews, L. *Inorg. Chem*. **1982**, *21*, 1519.
(33) Chen, J.; Dagdigian, P. J. *J. Chem. Phys.* **1992**, *96*, 7333.
(34) Brazier, C. R.; Ram, R. S.; Bernath, P. F. *J. Mol. Spectrosc*. **1986**, *120*, 381.
(35) Douglas, A. E.; Jones, W. E. *Can. J. Phys.* **1966**, *44*, 2251.
(36) Yamada, C.; Endo, Y.; Hirota, E. *J. Mol. Spectrosc*. **1986**, *117*, 134.
(37) Rinnenthal, J. L.; Gericke, K.-H. *J. Mol. Spectrosc*. **1999**, *198*, 115.
(38) Kobayashi, K.; Saito, S. *J. Chem. Phys.* **1998**, *108*, 6606.
(39) Kobayashi, K.; Goto, M.; Yamamoto, S.; Saito, S. *J. Chem. Phys.* **1996**, *104*, 8865.
(40) Woodman, C. M. *J. Mol. Spectrosc*. **1970**, *33*, 311.
(41) Xantheas, S. S.; Dunning, T. H., Jr.; Mavridis, A. *J. Chem. Phys.* **1997**, *106*, 3280.
(42) Bettendorff, M.; Peyerimhoff, S. D. *Chem. Phys.* **1986**, *104*, 29.
(43) Bettendorff, M.; Peyerimhoff, S. D. *Chem. Phys.* **1986**, *99*, 55.
(44) Rajendra, Pd.; Chandra, P. *J. Chem. Phys.* **2001**, *114*, 7450.
(45) Pritt, A. T., Jr.; Patel, D., Jr.; Coombe, R. D. *J. Mol. Spectrosc.* **1981**, *87*, 401.
(46) Pankratov, A. V.; Zercheninov, A. N.; Chesnokov, V. I.; Zhdanova, N. N. *Russ. J. Phys. Chem.* **1969**, *43*, 212.
(47) Chase, M. W., Jr.; Davies, C. A.; Downey, J. R., Jr.; Frurip, D. J.; McDonald, R. A.; Syverud, A. N. JANAF Thermochemical Tables (Supplement). *J. Phys. Chem. Ref. Data*. **1985**, *14*.
(48) Berkowitz, J.; Greene, J. P.; Foropoulos, J., Jr.; Neskovic, O. M. *J. Chem. Phys.* **1984**, *81*, 6166.
(49) Clyne, M. A. A.; MacRobert, A. *J. Chem. Soc., Faraday Trans. 2* **1983**, *79*, 283.
(50) Sloan, J. J.; Watson, D. G.; Wright, J. S. *Chem. Phys.* **1981**, *63*, 283.
(51) Gibson, S. T.; Greene, J. P.; Berkowitz, *J. Chem. Phys.* **1985**, *83*, 4319.
(52) Clark, T. C.; Clyne, M. A. A. *Trans. Faraday. Soc.* **1970**, *66*, 877.
(53) Habdas, J.; Wategaonkar, S. J.; Setser, D. W. *J. Phys. Chem.* **1987**, *91*, 451.
(54) Pellerite, M. J.; Jackson, R. L.; Brauman, J. I. *J. Phys. Chem.* **1981**, *85*, 1624.
(55) McMillen, D. F.; Golden, D. M. *Annu. Rev. Phys. Chem.* **1982**, *33*, 493.
(56) Baumgartel, H.; Jochims, H.-W.; Rühl, E.; Bock, H.; Dammel, R.; Minkwitz, J. Nass, R. *Inorg. Chem.* **1989**, *28*, 943.
(57) Srivatsava, A.; Arunan, E.; Manke, G., II; Setser, D. W.; Sumathi, R. *J. Phys. Chem. A.* **1998**, *102*, 6412.
(58) Toto, J. L.; Prichard, G. O.; Kirtman, B. *J. Phys. Chem.* **1994**, *98*, 8359 and references therein.
(59) Guo, J.-Z.; Deng, C.-H. *HueXue Wuli Xuebao (Chinese)* **1996**, *9*, 396.
(60) Jones, W. E. *Can. J. Phys.* **1967**, *45*, 21.